

## Future radioisotope measurements to clarify the origin of deep-ocean $^{244}\text{Pu}$

Xilu Wang,<sup>1,2,3,4</sup> Adam M. Clark,<sup>3</sup> John Ellis,<sup>5,6</sup> Adrienne F. Ertel,<sup>7,8</sup> Brian D. Fields,<sup>7,8,9</sup>  
 Brian J. Fry,<sup>10</sup> Zhenghai Liu,<sup>7,8,11</sup> Jesse A. Miller,<sup>7,8</sup> and Rebecca Surman<sup>3,4</sup>

<sup>1</sup>Key Laboratory of Particle Astrophysics, Institute of High Energy Physics,  
 Chinese Academy of Sciences, Beijing, 100049, China

<sup>2</sup>Department of Physics, University of California, Berkeley, CA 94720, USA

<sup>3</sup>Department of Physics, University of Notre Dame, Notre Dame, IN 46556, USA\*

<sup>4</sup>N3AS Collaboration

<sup>5</sup>Theoretical Physics and Cosmology Group, Department of Physics,  
 King's College London, Strand, London WC2R 2LS, UK

<sup>6</sup>NICPB, R vala pst. 10, 10143 Tallinn, Estonia; Theoretical Physics Department, CERN, CH-1211 Geneva 23, Switzerland

<sup>7</sup>Department of Astronomy, University of Illinois, Urbana, IL 61801, USA

<sup>8</sup>Illinois Center for the Advanced Study of the Universe, University of Illinois, Urbana, IL 61820, USA

<sup>9</sup>Department of Physics, University of Illinois, Urbana, IL 61801, USA

<sup>10</sup>Department of Physics, United States Air Force Academy, Colorado Springs, CO 80840, USA

<sup>11</sup>Department of Physics, North Carolina State University, Raleigh NC 27695, USA

$^{244}\text{Pu}$  has been discovered in deep-ocean deposits spanning the past 10 Myr, a period that includes two  $^{60}\text{Fe}$  pulses from nearby supernovae.  $^{244}\text{Pu}$  is among the heaviest  $r$ -process products, and we consider whether the  $^{244}\text{Pu}$  was created in the supernovae, which is disfavored by model calculations, or in an earlier kilonova that seeded  $^{244}\text{Pu}$  in the nearby interstellar medium, which was subsequently swept up by the supernova debris. We propose probing these possibilities by measuring other  $r$ -process radioisotopes such as  $^{129}\text{I}$  and  $^{182}\text{Hf}$  in deep-ocean deposits and in lunar regolith.

Measurements of live radioactive isotopes can provide insights into recent astrophysical explosions such as core-collapse supernovae (SNe) within  $\mathcal{O}(100)$  pc of Earth [1] that are expected to occur every few million years, clarifying the possibility of rarer events within  $\mathcal{O}(10)$  pc that might have caused mass extinctions in the past [2, 3]. Many experiments over the past two decades have detected pulses of live  $^{60}\text{Fe}$  in deep-ocean deposits [4–9] from between 2 and 3 My ago (Mya), very likely due to a nearby core-collapse SN. There have also been hints of earlier deep-ocean  $^{60}\text{Fe}$  deposition, as well as measurements of  $^{60}\text{Fe}$  in the lunar regolith [10], in cosmic rays [11] and in Antarctic snow [12].

In addition to these measurements, there have been some tantalizing hints of deep-ocean  $^{244}\text{Pu}$  [13–16]. These are interesting because the  $^{244}\text{Pu}$  would have been produced by the astrophysical  $r$ -process, whose likely sites include neutron-star mergers (kilonovae, KNe), and possibly some atypical SNe. Motivated by these hints, in a recent paper we studied possible signatures of SN and KN  $r$ -process events, analyzing the potential implications of  $^{244}\text{Pu}$  detection, estimating the strengths of other  $r$ -process radioisotope signatures, and discussing how they could help distinguish between potential sites [17].

A major advance in studies of live astrophysical radioisotopes has recently been made by Wallner *et al.* [18], who have discovered a second  $^{60}\text{Fe}$  pulse  $\sim 7$  Mya, as well as  $^{244}\text{Pu}$  in deep-ocean ferromagnetic crusts from periods that include both the  $^{60}\text{Fe}$  pulses. These results deepen greatly our picture of recent near-Earth explo-

sions, and widen dramatically the scope of their implications. Broadly, the second  $^{60}\text{Fe}$  pulse shows that there were multiple explosions, as one would expect from massive stars that are highly clustered [19]. And the detection of  $^{244}\text{Pu}$  not only is the second firmly detected radioisotope in this epoch, but also demands an  $r$ -process source and so probes the astrophysical site of the  $r$  process. In this paper we study the interpretation and potential implications of these new experimental results.

As has been shown in Fry *et al.* [20], ordinary non- $r$ -process) nucleosynthesis in core-collapse SNe provides the only plausible source of  $^{60}\text{Fe}$  observed in the two pulses. Wallner *et al.* [18] concur, making this a starting point of their analysis. The question then becomes: *could either or both of these SNe also have produced the  $^{244}\text{Pu}$ , or is a separate event required, presumably a KN?*

The two  $^{60}\text{Fe}$  pulses require two recent SNe. The  $^{244}\text{Pu}$  data were not sampled as finely in time as the  $^{60}\text{Fe}$  data:  $^{244}\text{Pu}$  was measured in three separate time windows, including a surface layer that probes anthropogenic contamination. The two deeper layers each overlap with a  $^{60}\text{Fe}$  pulse, as indicated by the yellow band in Fig. 1. The data show  $^{60}\text{Fe}$  to be much more abundant than  $^{244}\text{Pu}$  in both pulses.

SNe may produce the  $r$ -process via a  $\nu$ -driven wind or via magnetohydrodynamic (MHD) effects, but both struggle to make actinides, see [17] and references therein. If SNe are confirmed as robust sources of actinides such as  $^{244}\text{Pu}$ , the available models must have major omissions. We thus discussed in Wang *et al.* [17] a modified

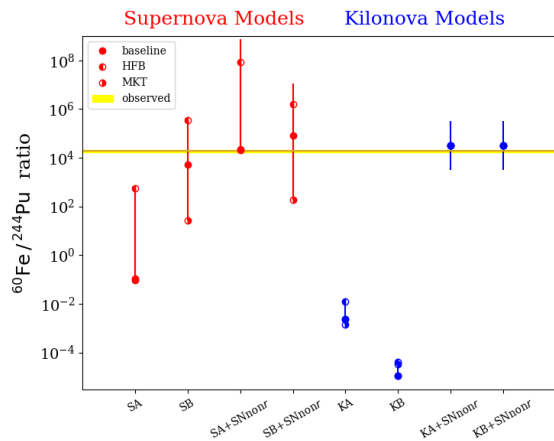


FIG. 1. The yellow band indicates the observed  ${}^{60}\text{Fe}/{}^{244}\text{Pu}$  ratio [18] for 3 Mya. We also show the  ${}^{60}\text{Fe}/{}^{244}\text{Pu}$  ratios calculated [17] in forced  $\nu$  wind and MHD SN models (SA and SB), and in KN models (KA and KB). We present results for each model both without and including an additional non- $r$ -process SN source of  ${}^{60}\text{Fe}$  at 100 pc; calculations are for events 3 Mya, but with a 10 Myr kilonova in the two-step KA/B+SNnonr models.

neutrino wind scenario *forced* to produce actinides and a high magnetic field MHD model, denoted by  $\nu^*$  (SA) and SB, respectively, which we constrained using data on the metal-poor star HD160617. We show in Fig. 1 results from these models, both without and including ordinary (non- $r$ -process) SN  ${}^{60}\text{Fe}$  production. Our calculations are made using the nuclear reaction network code Portable Routines for Integrated nucleoSynthesis Modeling (PRISM) [21, 22], as implemented in Wang *et al.* [17], with baseline nuclear data from [23] and [24] (FRDM+QRPA), and variations in the masses [25] (HFB),  $\beta$ -decay rates [26] (MKT), and fission yields [27]. The non- $r$ -process SN  ${}^{60}\text{Fe}$  yields are for an explosion at 100 pc with  $M_{\text{ej},60} \sim 10^{-4.5} M_{\odot}$  with an uncertainty discussed in the Supplemental Materials.

Neutron star mergers that lead to KN explosions are much rarer than SNe, but estimates of the KN rate in the Galaxy are compatible with a KN explosion  $\mathcal{O}(300)$  pc away that occurred  $\mathcal{O}(30)$  Mya. Accordingly, we also show in Fig. 1 results from two scenarios invoking a KN explosion 10 or 20 Mya, one a combination of calculations of dynamical ejecta and a disk  $\nu$ -driven wind (KA) constrained to fit data on HD160617, and the other a modified scenario (KB) that fits data on the actinide-boost star J0954+5246: both models are described in Wang *et al.* [17]. The KN  ${}^{60}\text{Fe}/{}^{244}\text{Pu}$  ratios span a large range ( ${}^{60}\text{Fe}/{}^{244}\text{Pu}_{\text{KN}} \sim 10^{-5}$  to  $10^{-2}$ ) when accounting for model uncertainties, but in the absence of an additional SN  ${}^{60}\text{Fe}$  source  ${}^{244}\text{Pu}$  is orders of magnitude *more* abundant than  ${}^{60}\text{Fe}$  in both models. This is because, whereas SNe expel  ${}^{60}\text{Fe}$  produced in multiple sites within the

event and its progenitor star, the outflows from a neutron star merger are expected to be sufficiently neutron-rich to progress robustly beyond the iron peak in the bulk of the ejecta.

We show in Fig 2 the uncertainties in these calculations found [17] using the nuclear data variations described above. We see again that either of the SN models SA or SB could accommodate the (similar)  ${}^{60}\text{Fe}/{}^{244}\text{Pu}$  ratios reported by [18] in the periods around 3 and 7 Mya. On the other hand, both the KN models KA and KB still predict much smaller  ${}^{60}\text{Fe}/{}^{244}\text{Pu}$  ratios, even when the uncertainties are taken into account. We therefore conclude that the  ${}^{60}\text{Fe}$  pulses and  ${}^{244}\text{Pu}$  detection *cannot be due to KN explosions alone*, at least as described by the models considered here.

We consider first the data of Wallner *et al.* [18] on the  ${}^{60}\text{Fe}$  pulse from  $\sim 3$  Mya. The timing of this signal is consistent with that measured previously in  ${}^{60}\text{Fe}$  deposits in deep-ocean sediments and crusts [4–9], though this peak is somewhat broader. A model in which  ${}^{60}\text{Fe}$  from a SN 100 Mpc away is transported to Earth in dust via ‘pinball’ trajectories that are deflected and trapped by a magnetic field within the SN remnant is compatible with a pulse of the observed size and duration  $\sim 1$  Myr [28], and the pulse width indicated by the Wallner *et al.* [18] measurements could also reflect smearing in the crust they study. Accordingly, we assume that this pulse was produced by a single SN, and assume that the  ${}^{244}\text{Pu}$  from  $\leq 4.57$  Mya measured by [18] is associated with this SN. We emphasize that observations with finer timing resolution would be needed to confirm this association, but note that many of our comments below would apply also if it were due to two or more SNe.

As discussed above, the additional  ${}^{60}\text{Fe}$  peak discovered by Wallner *et al.* [18], see also Fig. 1 of Fitoussi *et al.* [6], is likely due to another SN that occurred  $\sim 7$  Mya, also some  $\sim 100$  pc away. We assume that all the  ${}^{244}\text{Pu}$  from 4.57 to 9 Mya measured by Wallner *et al.* [18] is associated with this SN explosion, while emphasizing that observations with finer timing resolution would be needed to confirm this association. Under this assumption, the  ${}^{244}\text{Pu}/{}^{60}\text{Fe}$  ratios in the ejecta of the two SNe  $\sim 3$  and  $\sim 7$  Mya are comparable within a factor  $\sim 2$  and indistinguishable in Fig. 1.

This is intriguing, since simulations indicate that only very specific types of SN can make much  ${}^{244}\text{Pu}$  [17], in which case seeing two of them looks like a remarkable coincidence. If such an interpretation were correct, it would suggest not only that many or most SNe are  $r$ -process sites, but also that their production extends all the way to the actinides. If this could be established, standard  $\nu$ -driven wind and MHD models must have major omissions. However, actinide production is possible in the *forced* neutrino wind or MHD models  $\nu^*$  (SA) and SB discussed in Wang *et al.* [17].

As seen in Fig. 1, the artificially-enhanced SA model

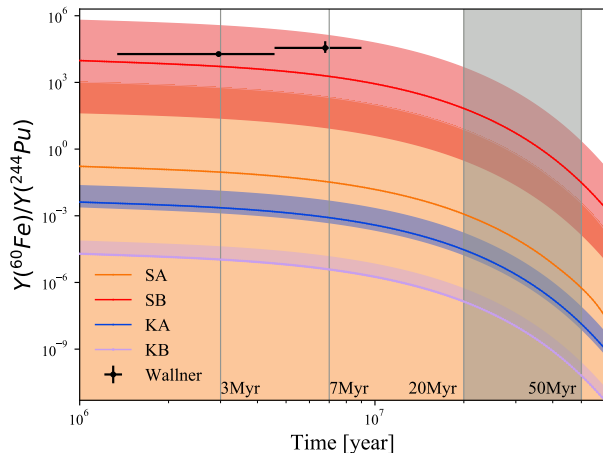


FIG. 2. The time evolution of the abundance ratio of  $^{60}\text{Fe}$  over  $^{244}\text{Pu}$  as calculated with the different astrophysical models described in Wang *et al.* [17]. The solid lines were obtained using our baseline  $r$ -process calculations, and the shaded bands (red: SA; orange: SB; light purple: KA; blue: KB) are the ranges due to uncertainties resulting from the adoption of different nuclear data, as described in the text. The vertical lines at 3 Mya and 7 Mya correspond to the identified nearby SNe Wallner *et al.* [18], and the shaded band between 20 and 50 Mya corresponds to the possibility of a prior KN. The black data points are the isotope ratios of  $^{60}\text{Fe}/^{244}\text{Pu}$  from periods  $\sim 3$  and 7 Mya measured by Wallner *et al.* [18].

overproduces  $^{244}\text{Pu}$  relative to  $^{60}\text{Fe}$ ! This could be brought into line with the data either by (1) including non- $r$ -process  $^{60}\text{Fe}$  production, or (2) with a smaller adjustment of the neutrino-driven wind, though this would still be incompatible with state-of-the-art SN models. The  $^{60}\text{Fe}/^{244}\text{Pu}$  ratio from the MHD SN model SB is compatible with the data, with or without non- $r$ -process  $^{60}\text{Fe}$  production.

However, serious potential issues for scenarios with actinide production in many or most SNe are provided by measurements of the  $r$ -process abundances in metal-poor stars. (a) It is known that  $r$ -process/Fe ratios (estimated using Eu/Fe as a proxy) vary wildly, with most stars showing low values and only a minority showing high values. The obvious interpretation is that Fe and  $r$ -process production are decoupled. If SNe do indeed make the  $r$ -process, one possibility would be that (core-collapse) supernova Fe production is highly variable. However, there are observational constraints on this from observations of SN light curves powered by  $^{56}\text{Ni}$  decay, so it seems more likely that the variations in  $r$ -process/Fe ratios are due to variations in  $r$ -process production. Another issue is that (b) searches for  $r$ -process species in metal-poor dwarf galaxies found them only in  $\sim 10\%$ . This strongly suggests that  $r$ -process events are much rarer than SNe. An alternative hypothesis is that the  $r$ -process material is ejected preferentially from the dwarf galaxies, e.g., in jets, but in this case jets would have to be features of

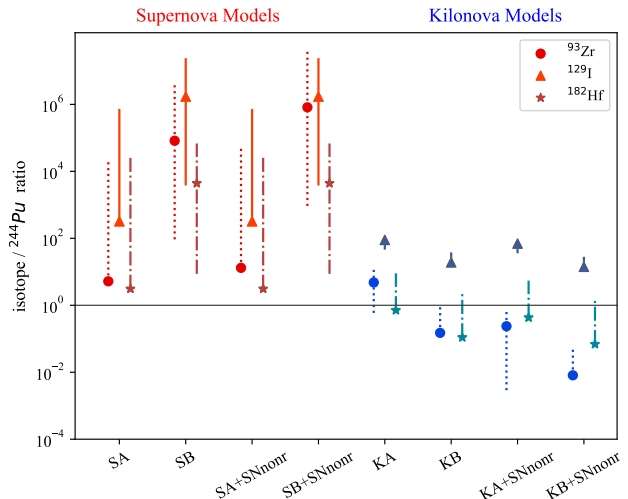


FIG. 3. Ratios to  $^{244}\text{Pu}$  of the selected live  $r$ -process radioisotopes  $^{93}\text{Zr}$ ,  $^{129}\text{I}$  and  $^{182}\text{Hf}$ , calculated in a similar way to Fig. 1.

most SNe, which is not supported by observations.

Motivated by these considerations, we proposed in Wang *et al.* [17] that  $^{244}\text{Pu}$  signals could arise via a two-step process in which material deposited previously in the interstellar medium (ISM) by an earlier KN was then swept up by subsequent SN explosions [29]. This hypothesis is consistent with the data shown in Fig. 1, and could explain naturally the similarity between the  $^{244}\text{Pu}/^{60}\text{Fe}$  ratios in the periods covering the two  $^{60}\text{Fe}$  pulses found by Wallner *et al.* [18] (see the Supplemental Material).

Any  $r$ -process mechanism that produces  $^{244}\text{Pu}$  also produces many other radioisotopes, not only other actinides such as  $^{236}\text{U}$ ,  $^{237}\text{Np}$ , and  $^{247}\text{Cm}$ , but also many other radioisotopes with masses intermediate between  $^{244}\text{Pu}$  and  $^{60}\text{Fe}$ . Hence their abundances would in general exhibit pulses coincident with the two SN  $^{60}\text{Fe}$  pulses. This feature would be independent of the  $r$ -process location, whether a recent, nearby SN or an earlier, more distant KN. However, the relative abundances of the peaks of different  $r$ -process isotopes would be affected by their lifetimes, which would help distinguish scenarios in which the  $r$ -process occurred at different times in the past.

We have calculated the relative abundances of live  $r$ -process radioisotopes produced by the *forced*  $\nu$ -wind (SA) and the MHD (SB) models for the SNe that occurred 3 Mya and 7 Mya discussed above, as well as the two scenarios for a KN explosion 10 or 20 Mya. Figure 3 compares the yields of selected live  $r$ -process radioisotopes predicted by our SN and KN models with direct deposition (one-step), and calculations for additional live  $r$ -process radioisotopes are tabulated in the Supplemental Material. We see that, if the  $^{244}\text{Pu}$  measured by Wallner *et al.* [18] was produced by a SN, one could hope to see accompanying  $^{93}\text{Zr}$ ,  $^{129}\text{I}$  and  $^{182}\text{Hf}$ .

Also shown in Fig. 3 are the  $^{93}\text{Zr}$ ,  $^{129}\text{I}$  and  $^{182}\text{Hf}/^{244}\text{Pu}$

ratios calculated in the two-step KN scenarios KA and KB, assuming that the KN occurred 10 Mya followed by a non- $r$ -process SN 3 Mya. We see that in both models and after both time lapses the  $^{129}\text{I}/^{244}\text{Pu}$  ratio exceeds unity, whereas the  $^{182}\text{Hf}/^{244}\text{Pu}$  ratios is smaller. The non- $r$ -process SN  $^{93}\text{Zr}$  yields are  $M_{\text{ej},93} \sim 10^{-7.5} M_{\odot}$  with an uncertainty discussed in the Supplemental Material.

It is a common feature of all the SN and KN models studied above that the best prospects for discovering a second live  $r$ -process radioisotope (in addition to  $^{244}\text{Pu}$ ) may be offered by  $^{129}\text{I}$ . The  $^{129}\text{I}/^{244}\text{Pu}$  ratio calculated in the models we have studied ranges from  $\mathcal{O}(10)$  in the KN models through  $\mathcal{O}(100)$  in SN model SA to  $\mathcal{O}(10^6)$  in SN model SB, thereby offering the possibility of distinguishing between scenarios. An  $^{129}\text{I}/^{244}\text{Pu}$  ratio exceeding  $10^5$  coincident with either of the observed SN pulses would favour SN model SB, which would also predict  $^{182}\text{Hf}/^{244}\text{Pu}$  ratios  $> 10^3$ . On the other hand, a  $^{129}\text{I}/^{244}\text{Pu}$  ratio between  $10^3$  and 10 could be accommodated by any of the models SA, KA and KB. In this case, model SA suggests that  $^{182}\text{Hf}$  might be present at levels similar to  $^{244}\text{Pu}$ , whereas the KN models predict smaller ratios for  $^{182}\text{Hf}$  relative to  $^{244}\text{Pu}$ , that are less likely to be detectable. Hence, detection of  $^{182}\text{Hf}$  at a level similar to  $^{244}\text{Pu}$  would point strongly towards a SN  $r$ -process origin. Additionally, detection of any of the other  $r$ -process radioisotopes  $^{93}\text{Zr}$ ,  $^{107}\text{Pd}$ ,  $^{135}\text{Cs}$ ,  $^{182}\text{Hf}$ ,  $^{237}\text{Np}$  or  $^{247}\text{Cm}$  would favour a SN origin for the  $^{244}\text{Pu}$ , whereas  $^{236}\text{U}$  detection is possible in both SN and KN scenarios.

There are also possible signatures of nearby explosions in cosmic rays, including anomalies in positron and antiproton fluxes [30], and also in the ion composition. Indeed,  $^{60}\text{Fe}$  is seen in cosmic rays [11], and anomalies in elemental iron fluxes at low energies also suggest a perturbation due to a recent event [31]. A nearby  $r$ -process event would mainly produce stable isotopes, which would be difficult to identify in deposits on the Earth or Moon, but might be detectable among the cosmic rays. Indeed, SuperTIGER measurements of cosmic-ray elemental composition have recently reported [32, 33] that elements with  $42 \leq Z \leq 54$  show anomalously high abundances. These heavy elements exceed the levels of a mix of 80% solar-system abundances with a 20% admixture of supernova winds and ejecta that fits lower-mass cosmic-ray species. Some of these anomalous elements are produced mainly by the  $r$ -process, though with admixtures of  $s$ -process production. Intriguingly, the dominantly  $s$ -process species barium is not as enhanced as the other high- $Z$  elements, which may be circumstantial support for the hypothesis of a nearby  $r$ -process site [33]. Cosmic-ray measurements of other  $r$ -process species such as actinides could shed light on the nucleosynthesis pattern and thus the  $r$ -process source. If isotopic measurement were possible in future cosmic-ray experiments, observation of  $^{182}\text{Hf}$  would be particularly interesting, since it should not have significant contamination from spalla-

tion of neighboring nuclides.  $^{129}\text{I}$  and  $^{135}\text{Cs}$  would also be of interest, though contamination from spallation of Te, Xe, and Ba may be an issue.

We now consider the possibility of observing additional SNe pulses in deep-ocean deposits from  $> 7$  Mya. A model of the Local Bubble and  $^{60}\text{Fe}$  transport proposed in [34, 35] postulates 14 to 20 SNe in the Scorpio-Centaurus (Sco-Cen) stellar association within 300 pc over the past 13 My, among which might be progenitors for the two observed  $^{60}\text{Fe}$  pulses. Ref. [18] reported the results of  $^{60}\text{Fe}$  searches extending over the past 10 My, finding that the signal-to-background ratio for  $^{60}\text{Fe}$  falls to around unity for deposits from between 7 and 10 Mya. The relatively short  $^{60}\text{Fe}$  half-life of 2.6 My would make searches for earlier  $^{60}\text{Fe}$  pulses even more challenging. On the other hand, indirect evidence for earlier SNe could come from pulses of swept-up  $^{244}\text{Pu}$  in earlier deep-ocean deposits, in view of its much longer half-life  $\sim 80$  My. Ref. [16] reported the results of a search for  $^{244}\text{Pu}$  extending over the past 25 My, finding one event from  $> 12$  Mya. This event might just be background, but if not would correspond to a rate of deposition similar to that between 5 and 12 Mya. The more sensitive  $^{244}\text{Pu}$  results of Wallner *et al.* [18] extend back to 9 Mya, and it would clearly be interesting to extend the search for an earlier  $^{244}\text{Pu}$  signal and any possible time structure. A prime  $r$ -process candidate for corroborating any another  $^{244}\text{Pu}$  peak would again be  $^{129}\text{I}$ , in view of the production rates found in both SN and KN models and its favourable half-life  $\sim 16$  My.

We close with some remarks about searches for live  $r$ -process radioisotopes in samples of lunar regolith. We recall that Fimiani *et al.* [10] have reported the discovery of  $^{60}\text{Fe}$  in several *Apollo* samples. The data of Wallner *et al.* [18] suggest that this  $^{60}\text{Fe}$  is likely to have originated from a combination of the  $^{60}\text{Fe}$  pulses from 3 and 7 Mya, mainly the more recent pulse, in view of its greater size and younger age. Confirmation of this  $^{60}\text{Fe}$  signal, e.g., in the sample returned recently by the *Chang'e-5* mission [36] or that from a future *Artemis* mission [37], would require analyzing a modest sample of  $\lesssim 100$  mg of lunar material [38]. The relative abundance of  $^{244}\text{Pu}$  reported by [18] is  $\sim 5 \times 10^{-5}$ , suggesting that several kg of lunar regolith might be needed to discover a  $^{244}\text{Pu}$  signal. On the other hand, a much smaller sample might be sufficient to detect an  $^{129}\text{I}$  signal, since the  $^{129}\text{I}/^{244}\text{Pu}$  ratio is predicted to lie in the range  $\mathcal{O}(10)$  (for the KN models) through  $\mathcal{O}(100)$  (for SN model SA) to  $\mathcal{O}(10^6)$  (for SN model SB).

The AMS sensitivity for  $^{129}\text{I}$  already reaches the needed level, but the challenge is to avoid contamination from anthropogenic sources.  $^{129}\text{I}$  has already been measured in a Fe-Mn crust [39], showing a dropoff with depth consistent with a background source such as natural uranium fission. The FeMn crust is not independently dated, but the abundance levels appear inconsistent with the SB

model while allowing room for some SA models and the KA and KB models. We note that Nishiizumi *et al.* [40] used accelerator mass spectrometry to measure  $^{129}\text{I}$  in the lunar regolith, and Nishiizumi *et al.* [41] measured it in lunar rock, finding very similar abundances. These data foreshadow the power of new radioisotope measurements on both terrestrial and lunar samples, particularly  $^{129}\text{I}$  and  $^{182}\text{Hf}$ , which can probe the nature of the recent explosions and of the  $r$ -process generally.

We are grateful for illuminating discussions with Terri Brandt and Brian Rauch about SuperTIGER and cosmic rays, and to Toni Wallner and Dominik Koll for discussions of their work. X.W., R.S., and B.D.F. acknowledge many useful discussions in the INT-21-3 workshop on cosmic radioisotopes sponsored by the Institute for Nuclear Theory. The work of X.W. was supported by the U.S. National Science Foundation (NSF) under grants No. PHY-1630782 and PHY-2020275 for the Network for Neutrinos, Nuclear Astrophysics, and Symmetries (N3AS) and by the Heising-Simons Foundation under award 00F1C7. The work of A.M.C. was supported by the U.S. Nuclear Regulatory Committee Award 31310019M0037 and the National Science Foundation under grant number PHY-2011890. The work of J.E. was supported partly by the United Kingdom STFC Grant ST/T000759/1 and partly by the Estonian Research Council via a Mobilitas Pluss grant. The work of A.F.E. and B.D.F. was supported by the NSF under grant number AST-2108589. The work of J.A.M. was supported by the Future Investigators in NASA Earth and Space Science and Technology (FINESST) program under grant number NNN19ZDA001N-FINESST. The work of R.S. was supported by N3AS as well as the U.S. Department of Energy under Nuclear Theory Contract No. DE-FG02-95-ER40934.

---

\* wangxl@ihep.ac.cn; xlwang811@gmail.com

- [1] J. Ellis, B. D. Fields, and D. N. Schramm, *Astrophys. J.* **470**, 1227 (1996), arXiv:astro-ph/9605128 [astro-ph].
- [2] M. A. Ruderman, *Science* **184**, 1079 (1974).
- [3] J. Ellis and D. N. Schramm, *Proceedings of the National Academy of Sciences* **92**, 235 (1995), <https://www.pnas.org/content/92/1/235.full.pdf>.
- [4] K. Knie, G. Korschinek, T. Faestermann, C. Wallner, J. Scholten, and W. Hillebrandt, *Phys. Rev. Lett.* **83**, 18 (1999).
- [5] K. Knie *et al.*, *Phys. Rev. Lett.* **93**, 171103 (2004).
- [6] C. Fitoussi *et al.*, *Phys. Rev. Lett.* **101**, 121101 (2008), arXiv:0709.4197 [astro-ph].
- [7] A. Wallner *et al.*, *Nature* **532**, 69 (2016).
- [8] P. Ludwig, S. Bishop, R. Egli, V. Chernenko, B. Deneva, T. Faestermann, N. Famulok, L. Fimiani, J. M. Gómez-Guzmán, K. Hain, G. Korschinek, M. Hanzlik, S. Merchel, and G. Rugel, *Proceedings of the National Academy of Sciences* **113**, 9232 (2016), <https://www.pnas.org/content/113/33/9232.full.pdf>.
- [9] A. Wallner, J. Feige, L. K. Fifield, M. B. Froehlich, R. Golser, M. A. C. Hotchkis, D. Koll, G. Leckenby, M. Martschini, S. Merchel, S. Panjkov, S. Pavetich, G. Rugel, and S. G. Tims, *Proceedings of the National Academy of Science* **117**, 21873 (2020).
- [10] L. Fimiani *et al.*, *Phys. Rev. Lett.* **116**, 151104 (2016).
- [11] W. Binns *et al.*, *Science* **352**, 677 (2016).
- [12] D. Koll, G. Korschinek, T. Faestermann, J. Gómez-Guzmán, S. Kipfstuhl, S. Merchel, and J. M. Welch, *Phys. Rev. Lett.* **123**, 072701 (2019).
- [13] M. Paul, A. Valenta, I. Ahmad, D. Berkovits, C. Bordenau, S. Ghelberg, Y. Hashimoto, A. Hershkovitz, S. Jiang, T. Nakanishi, and K. Sakamoto, *ApJL* **558**, L133 (2001), arXiv:astro-ph/0106205 [astro-ph].
- [14] C. Wallner, T. Faestermann, U. Gerstmann, K. Knie, G. Korschinek, C. Lierse, and G. Rugel, *New Astronomy Reviews* **48**, 145 (2004).
- [15] G. Raisbeck, T. Tran, D. Lunney, C. Gaillard, S. Goriely, C. Waelbroeck, and F. Yiou, *Nuclear Instruments and Methods in Physics Research B* **259**, 673 (2007).
- [16] A. Wallner, T. Faestermann, J. Feige, C. Feldstein, K. Knie, G. Korschinek, W. Kutschera, A. Ofan, M. Paul, F. Quinto, G. Rugel, and P. Steier, *Nature Communications* **6**, 5956 (2015), arXiv:1509.08054 [astro-ph.SR].
- [17] X. Wang, A. M. Clark, J. Ellis, A. F. Ertel, B. D. Fields, Z. Liu, J. A. Miller, and R. Surman, “ $r$ -Process Radioisotopes from Near-Earth Supernovae and Kilonovae,” (2021), arXiv:2105.05178 [astro-ph.HE].
- [18] A. Wallner *et al.*, *Science* **372**, 742 (2021).
- [19] H. Zinnecker and H. W. Yorke, *ARA&A* **45**, 481 (2007), arXiv:0707.1279 [astro-ph].
- [20] B. J. Fry, B. D. Fields, and J. R. Ellis, *Astrophys. J.* **800**, 71 (2015), arXiv:1405.4310 [astro-ph.SR].
- [21] M. R. Mumpower, T. Kawano, T. M. Sprouse, N. Vassh, E. M. Holmbeck, R. Surman, and P. Möller, *Astrophys. J.* **869**, 14 (2018), arXiv:1802.04398 [nucl-th].
- [22] T. M. Sprouse, M. R. Mumpower, and R. Surman, arXiv e-prints (2020), arXiv:2008.06075 [nucl-th].
- [23] P. Möller, A. J. Sierk, T. Ichikawa, and H. Sagawa, *At. Data Nucl. Data Tables* **109**, 1 (2016), arXiv:1508.06294 [nucl-th].
- [24] P. Möller, M. R. Mumpower, T. Kawano, and W. D. Myers, *At. Data Nucl. Data Tables* **125**, 1 (2019).
- [25] S. Goriely, N. Chamel, and J. M. Pearson, *Phys. Rev. Lett.* **102**, 152503 (2009), arXiv:0906.2607 [nucl-th].
- [26] T. Marketin, L. Huther, and G. Martinez-Pinedo, *Phys. Rev. C* **93**, 025805 (2016).
- [27] T. Kodama and K. Takahashi, *Nuclear Physics A* **239**, 489 (1975).
- [28] B. J. Fry, B. D. Fields, and J. R. Ellis, *Astrophys. J.* **894**, 109 (2020), arXiv:1801.06859 [astro-ph.HE].
- [29] First estimates of the possible amounts of swept-up  $^{60}\text{Fe}$  and  $^{244}\text{Pu}$  were given in Ellis *et al.* [1].
- [30] M. Kachelrieß, A. Neronov, and D. V. Semikoz, *Phys. Rev. D* **97**, 063011 (2018), arXiv:1710.02321 [astro-ph.HE].
- [31] M. J. Boschini, S. Della Torre, M. Gervasi, D. Grandi, G. Jóhannesson, G. La Vacca, N. Masi, I. V. Moskalenko, S. Pensotti, T. A. Porter, L. Quadrani, P. G. Rancoita, D. Rozza, and M. Tacconi, *Astrophys. J.* **913**, 5 (2021), arXiv:2101.12735 [astro-ph.HE].
- [32] N. E. Walsh *et al.*, *PoS ICRC2021*, 118 (2021).
- [33] N. E. Walsh, *Washington University Arts & Sciences Electronic Theses and Dissertations* **2251** (2020), <https://doi.org/10.7936/42be-8069>.

- [34] D. Breitschwerdt, J. Feige, M. M. Schulreich, M. A. D. Avillez, C. Dettbarn, and B. Fuchs, *Nature (London)* **532**, 73 (2016).
- [35] M. M. Schulreich, D. Breitschwerdt, J. Feige, and C. Dettbarn, *Astron. Astrophys.* **604**, A81 (2017), [arXiv:1704.08221](https://arxiv.org/abs/1704.08221) [astro-ph.HE].
- [36] Y. Qian, L. Xiao, Q. Wang, J. W. Head, R. Yang, Y. Kang, C. H. van der Bogert, H. Hiesinger, X. Lai, G. Wang, Y. Pang, N. Zhang, Y. Yuan, Q. He, J. Huang, J. Zhao, J. Wang, and S. Zhao, *Earth and Planetary Science Letters* **561**, 116855 (2021).
- [37] M. Smith, D. Craig, N. Herrmann, E. Mahoney, J. Krezel, N. McIntyre, and K. Goodliff, in *2020 IEEE Aerospace Conference* (2020) pp. 1–10.
- [38] Employing the regolith gardening model of [? ?], it is estimated in [36] that the depth  $\Lambda$  at which the probability of at least one overturn is 99% is  $3.45 \times 10^{-5} t_{\text{yr}}^{0.47}$  m, where  $t_{\text{yr}}$  is the reworking time in years. This leads to  $\Lambda = 3.8$  (5.7) cm for material deposited 3 (7) Mya.
- [39] L. Ji, G. Liu, Z. Chen, Y. Huang, N. Xing, S. Jiang, and M. He, *Acta Oceanologica Sinica* **34**, 31 (2015).
- [40] K. Nishiizumi, P. W. Kubik, P. Sharma, and J. R. Arnold, in *52nd Annual Meeting of the Meteoritical Society*, Vol. 52 (1989) p. 179.
- [41] K. Nishiizumi, D. Elmoro, M. Honda, J. R. Arnold, and H. E. Gove, *Nature (London)* **305**, 611 (1983).
- [42] R. Diehl, M. Lugaro, A. Heger, A. Sieverding, X. Tang, K. Li, E. Li, C. L. Doherty, M. G. H. Krause, A. Wallner, N. Prantzos, H. E. Brinkman, J. W. den Hartogh, B. Wehmeyer, A. Yagüe López, M. M. M. Pleintinger, P. Banerjee, and W. Wang, *arXiv e-prints* (2021), [arXiv:2109.08558](https://arxiv.org/abs/2109.08558) [astro-ph.HE].
- [43] K. Rozwadowska, F. Vissani, and E. Cappellaro, *New Astronomy* **83**, 101498 (2021), [arXiv:2009.03438](https://arxiv.org/abs/2009.03438) [astro-ph.HE].
- [44] T. Sukhbold, T. Ertl, S. E. Woosley, J. M. Brown, and H. T. Janka, *Astrophys. J.* **821**, 38 (2016), [arXiv:1510.04643](https://arxiv.org/abs/1510.04643) [astro-ph.HE].
- [45] M. Limongi and A. Chieffi, *ApJS* **237**, 13 (2018), [arXiv:1805.09640](https://arxiv.org/abs/1805.09640) [astro-ph.SR].
- [46] S. Curtis, K. Ebinger, C. Fröhlich, M. Hempel, A. Perego, M. Liebendörfer, and F.-K. Thielemann, *Astrophys. J.* **870**, 2 (2019), [arXiv:1805.00498](https://arxiv.org/abs/1805.00498) [astro-ph.SR].

## SUPPLEMENTAL MATERIAL

The first four columns of Table I compare the yields of live  $r$ -process radioisotopes predicted by SN models SA and SB for SNe that exploded 3 and 7 Mya. We emphasize that the  $^{60}\text{Fe}/^{244}\text{Pu}$  ratios given in this Table are only for  $^{60}\text{Fe}$  produced via the  $r$ -process, and that we would expect these SNe to produce much more  $^{60}\text{Fe}$  via the standard neutron capture mechanism. If the  $^{244}\text{Pu}$  measured in [18] was produced by such a SN, one could hope to see accompanying signals of  $r$ -process production of the radioisotopes  $^{93}\text{Zr}$ ,  $^{107}\text{Pd}$ ,  $^{129}\text{I}$ ,  $^{135}\text{Cs}$ ,  $^{182}\text{Hf}$  and  $^{236}\text{U}$ , and possibly  $^{237}\text{Np}$  and  $^{247}\text{Cm}$ . However, in order to detect all these signals, better time resolution would be needed.

Table I show results from calculations of  $r$ -process iso-

tope production in KN models KA and KB, assuming an event 10 or 20 Mya, bracketing the formation of the Local Bubble. In this case many of the shorter-lived radioisotopes that could have been detectable in the case of a more recent SN would have decayed away, and we find that if the measured  $^{244}\text{Pu}$  was produced by a KN 10 or 20 Mya, the best prospects for detection are for  $^{129}\text{I}$ , followed by  $^{236}\text{U}$ . There may also be some prospects for detection of  $^{107}\text{Pd}$ , for  $^{182}\text{Hf}$  in model KA, and for  $^{93}\text{Zr}$  in model KA if the explosion occurred 10 Mya.

In the main text and in Figure 3 we highlight representative isotopes in each of the three regions of the  $r$ -process abundance pattern: namely  $^{93}\text{Zr}$ ,  $^{129}\text{I}$ , and  $^{182}\text{Hf}$ . We anticipate  $^{182}\text{Hf}$  to be a clear marker of prompt supernova production, as it is present in potentially detectable levels for the SA and SB models but not in the two-step kilonova scenarios.  $^{93}\text{Zr}$  can be produced in an alpha-rich freezeout of mildly neutron-rich supernova ejecta without an accompanying main  $r$ -process, so its detection could be a probe of this additional nucleosynthetic source. Our predictions show  $^{129}\text{I}$  should be detectable alongside  $^{244}\text{Pu}$  in any scenario, with the measured ratio offering possibly the strongest evidence to discriminate between scenarios. The other radioisotopes in the Table could provide similar insights into the  $r$ -process, if they could be measured.

Our predictions for radioisotope ratios to  $^{244}\text{Pu}$  in Figs. 1 and 3 include results that combine  $r$ -process yields with those from ordinary (non- $r$ -process) supernova explosions. This requires absolute mass yields (not just ratios) of  $^{244}\text{Pu}$  and  $^{60}\text{Fe}$ , which are implemented as follows. We adopt the [17] estimate for the total kilonova  $r$ -process yields:  $M_{\text{ej},r}(\text{KA},\text{KB}) = (1.76 \times 10^{-2}, 7.00 \times 10^{-3})M_{\odot}$ . The  $^{244}\text{Pu}$  mass yield is then  $M_{\text{ej},244} = A_{244}Y_{244}M_{\text{ej},r}$ .

Gamma-ray line observations give an observational indication of the mean  $^{60}\text{Fe}$  yield. Given a Galactic steady-state  $^{60}\text{Fe}$  mass  $M_{60,ss} = 2.85 M_{\odot}$  [42], and a core-collapse supernova rate  $R_{\text{SN}} = 1.7$  events/century [43], the mean  $^{60}\text{Fe}$  yield is  $M_{\text{ej},60} = M_{60,ss}/\tau_{60}R_{\text{SN}} = 4.5 \times 10^{-5} M_{\odot}$  where  $\tau_{60}$  is the  $^{60}\text{Fe}$  lifetime; the uncertainty in this mean yield is at least a factor of 2. Supernova nucleosynthesis calculations suggest that  $^{60}\text{Fe}$  yields span a wide range, varying both sensitively and non-monotonically with progenitor mass. Yields in ref. [44] lie in the range  $(4 \times 10^{-6}, 3 \times 10^{-4})M_{\odot}$ , which includes the calculations of [45] and model w of [46]. We thus adopt a  $^{60}\text{Fe}$  yield of  $M_{\text{ej},60} = 10^{-4.5 \pm 1} M_{\odot}$ . Similarly, the yields of  $^{93}\text{Zr}$  from ordinary (non- $r$ -process) supernova explosions are in the range  $(1.4 \times 10^{-9}, 2.4 \times 10^{-7})M_{\odot}$  (from [45] and model w of [46]), thus a  $^{93}\text{Zr}$  yield of  $M_{\text{ej},93} = 10^{-7.5 \pm 1} M_{\odot}$  is adopted.

The measured  $^{60}\text{Fe}/^{244}\text{Pu} = F_{60}/F_{244}$  ratio reflects the fluence ratio. For  $^{244}\text{Pu}$  we use the observed interstellar  $^{244}\text{Pu}$  flux to determine the fluence  $F_{244} = \Phi_{244}^{\text{interstellar}} \Delta t$ , where  $\Delta t$  is the timespan of the mea-

TABLE I. *r*-process isotope ratios in forced SN models for explosions 3/7 Mya, corresponding to the known  $^{60}\text{Fe}$  pulses, and in KN models for explosions 10/20 Mya, bracketing the formation of the Local Bubble.

Radioisotope Ratio	Supernova Models				Kilonova Models			
	SA		SB		KA		KB	
	3 Mya	7 Mya	3 Mya	7 Mya	10 Mya	20 Mya	10 Mya	20 Mya
$^{60}\text{Fe}/^{244}\text{Pu}$	$9.2 \times 10^{-2}$	$3.2 \times 10^{-2}$	$5.3 \times 10^3$	$1.8 \times 10^3$	$3.7 \times 10^{-4}$	$3.0 \times 10^{-5}$	$1.7 \times 10^{-6}$	$1.4 \times 10^{-7}$
$^{93}\text{Zr}/^{244}\text{Pu}$	5.2	0.93	$8.2 \times 10^4$	$1.5 \times 10^4$	0.24	$3.6 \times 10^{-3}$	$7.7 \times 10^{-3}$	$1.2 \times 10^{-4}$
$^{107}\text{Pd}/^{244}\text{Pu}$	52	35	$1.3 \times 10^5$	$8.6 \times 10^4$	3.7	1.4	0.34	0.13
$^{129}\text{I}/^{244}\text{Pu}$	$3.2 \times 10^2$	$2.8 \times 10^2$	$1.7 \times 10^6$	$1.5 \times 10^6$	69	49	14	10
$^{135}\text{Cs}/^{244}\text{Pu}$	5.4	0.68	$1.2 \times 10^5$	$1.5 \times 10^4$	$8.7 \times 10^{-3}$	$5.5 \times 10^{-5}$	$3.7 \times 10^{-2}$	$2.4 \times 10^{-4}$
$^{182}\text{Hf}/^{244}\text{Pu}$	3.1	2.3	$4.4 \times 10^3$	$3.3 \times 10^3$	0.43	0.22	$6.9 \times 10^{-2}$	$3.5 \times 10^{-2}$
$^{236}\text{U}/^{244}\text{Pu}$	1.8	1.7	9.5	8.7	1.8	1.5	1.0	0.92
$^{237}\text{Np}/^{244}\text{Pu}$	0.66	0.18	1.6	0.43	$8.2 \times 10^{-2}$	$3.7 \times 10^{-3}$	$5.6 \times 10^{-2}$	$2.5 \times 10^{-3}$
$^{247}\text{Cm}/^{244}\text{Pu}$	0.50	0.43	0.45	0.39	0.38	0.27	0.35	0.25

surement interval. The *r*-process contribution to  $^{60}\text{Fe}$  then follows as  $F_{60,r} = f_{\text{Fe}}/f_{\text{Pu}} ({}^{60}\text{Fe}/{}^{244}\text{Pu})_r F_{244}$ , where  $({}^{60}\text{Fe}/{}^{244}\text{Pu})_r$  is the model ratio, and we take the ra-

tio of dust fractions to be  $f_{\text{Fe}}/f_{\text{Pu}} = 1$ . For the ordinary (non-*r*-process) supernova  $^{60}\text{Fe}$  fluence, we use  $F_{\text{non-}r,60} = f_{\text{Fe}} M_{\text{ej},60} / 16\pi A_{60} m_u r_{\text{SN}}^2$ , where we take the dust fraction  $f_{\text{Fe}} = 0.1$ , and use  $r_{\text{SN}} = 100$  pc.